Comparing frustrated and unfrustrated clusters of single-domain ferromagnetic islands

J. Li,[1] S. Zhang,[1] J. Bartell,[1] C. Nisoli,[2] X. Ke,[3] Paul E. Lammert,[1] Vincent H. Crespi,[1] and P. Schiffer[1,*]
[1]*Department of Physics and Materials Research Institute, Pennsylvania State University, University Park, Pennsylvania 16802, USA*
[2]*Theoretical Division and Center for Nonlinear Studies, Los Alamos National Laboratory, Los Alamos, New Mexico 87545, USA*
[3]*Neutron Scattering Science Division, Oak Ridge National Laboratory, Oak Ridge, Tennessee 37831, USA*
(Received 28 July 2010; revised manuscript received 7 September 2010; published 5 October 2010)

We have studied the magnetic-moment configurations of different geometry clusters of single-domain nanoscale ferromagnetic islands. The clusters consisted of four islands arranged in geometries taken from the square lattice of artificial spin ice. The magnetic-moment configurations were imaged by magnetic force microscopy after effectively annealing through ac demagnetization. We then compared the results for cluster geometries with and without frustration of the magnetostatic interactions between the island moments. We found that nonfrustrated clusters achieve their lowest energy states more readily than do frustrated clusters. This behavior suggests the presence of a kinetic barrier associated with frustration of the magnetostatic interactions.

DOI: 10.1103/PhysRevB.82.134407 PACS number(s): 75.50.Lk, 75.75.−c

Recent investigations of single-domain ferromagnets lithographically defined into frustrated arrays have provided insights into the nature of geometrical frustration. Square,[1–10] hexagonal,[8,9,11–15] triangular,[16,17] and brickwork[7] arrays have been examined both theoretically and experimentally. The square arrays have perpendicular nearest neighbors in which the moment orientation resembles the two-in/two-out spin ice ground state of pyrochlore materials.[1,2,18] The hexagonal geometry resembles the one-in/two-out or two-in/one-out quasi-ice state of the well-known kagome lattice.[11–13] Clusters consisting of excerpts from the kagome lattice have also been investigated by photoemission electron microscopy,[19] obtaining weaker moment optimization in larger clusters. In a related line of work, complex clusters of magnetostatically interacting ferromagnetic islands have recently shown the ability to propagate information[20] and realize a logic functionality[21,22] through application of a clock field.

Since the geometries of artificially frustrated magnets are defined lithographically, the lattice geometry and interaction strength can be controlled. This allows the experimental investigation of statistical models, such as the two-dimensional Ising model and various vertex models.[23,24] Under certain conditions, the moment configurations of these systems in a demagnetized state can be described through an effective thermodynamic formalism, even though the moment interactions are athermal.[4,9] The precise kinetics of the moments during application of an external field remains unclear, however, because of the complexity of the micromagnetics and the complex magnetostatic energy landscape.

In the present work, we study a simplified system: island clusters containing only four magnetostatically interacting moments. We examine the energetics and moment configurations of 15 cluster geometries either with frustration (F) or without frustration (NF) in the near-neighbor magnetostatic interactions between island moments. This range of geometries allows us to explore the nature of different fourfold correlations types without the constraint of the surrounding islands. We find that isolated clusters more readily reach their low-energy states than the same configurations of islands embedded within a larger array. Furthermore, cluster geometries in which the interactions are not frustrated are better able to reach their ground states than frustrated geometry clusters, indicating that frustration in itself impedes energy minimization in the cluster geometry.

We lithographically fabricated 15 geometrically distinct types of isolated clusters, each consisting of four identical ferromagnetic Permalloy islands (220 nm × 80 nm lateral and 25 nm thick) following procedures published previously.[2] The island magnetic moments are constrained to point along their long axes due to strong shape anisotropy, similar to Ising spins. The coercivity of islands with these dimensions is ~770 Oe and does not depend significantly on the island-island interactions.[3] These clusters are fragments of the square artificial spin ice lattice that we have previously studied extensively, and the particular clusters are chosen as relatively compact groups of four islands from within that lattice. The nearest along-axis center-to-center spacing of islands within a cluster was 400 nm for most of the data presented [see Fig. 1(a)], although we also examined other spacings to vary the strength of the interisland interactions. Different clusters were separated by at least 2 μm edge-to-edge distance to avoid intercluster interactions. Populations of 5000 to 10 000 clusters for each of the 15 types are fabricated on the same substrate with the same orientation, with distinct cluster types being separated by at

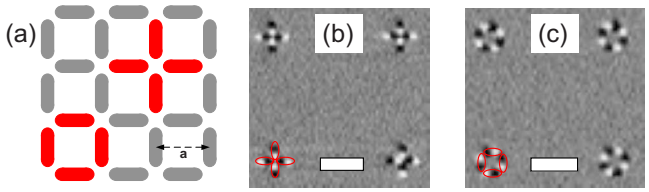

FIG. 1. (Color online) (a) Extraction of two clusters F1 (upper right) and NF6 (lower left) from a square artificial spin ice lattice, the lattice spacing, a, is defined as indicated; (b) and (c) show the MFM images of cluster F1 (cross) and cluster NF6 (loop), respectively, where the scale bar is 1 μm.

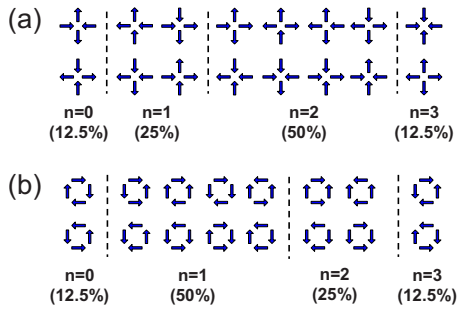

FIG. 2. (Color online) The symmetry-distinct classes of moment microstates (i.e., distinct energy states) for (a) geometry F1 (crosslike cluster) and (b) geometry NF6 (looplike cluster); The percentages indicate the expected fraction of each state if the individual moment orientations were completely random.

least 100 μm. Each data point shown below is obtained by averaging data from between 360 and 640 individual clusters.

Because the energy scales of magnetostatic interaction in these systems are roughly 10^3 times higher than room-temperature thermal energies,[2] we enable the island moments to access low-energy states through a process of ac demagnetization developed previously.[1,2] Following our previously developed protocol, the samples are rotated in plane while subject to a stepwise deceasing in-plane external field with field polarity within the laboratory frame reversed at each step.[1–3] Initially, the external field is strong enough to coerce all island moments into tracking the field. As the strength of the external field decreases, island moments successively decouple from the field, as guided by the local magnetostatic interactions. The rotational demagnetization protocol allows the clusters to explore microstates in the spin-configuration space wherein each island moment makes one ultimate decision on its configuration relative to nearby islands.

In previous work we demonstrated that the final vertex energy of our arrays could be reduced by reducing the magnetic step size in our rotational demagnetization but the minimum attainable magnetostatic energy for the extended square lattices was still well above the ground-state energy.[1,4,7] In the present work, we used the minimum practical step size of 1.6 Oe (in extended lattices, this step size led to nearly the same energy one would obtain by extrapolating to zero step size). After ac demagnetization, the island magnetic moments were imaged via magnetic force microscopy (MFM) at several locations on each array of clusters, imaging typically 100 clusters per MFM scan. Figures 1(b) and 1(c) show MFM images of two geometries, the F1 (cross) and NF6 (loop) clusters, with white and black contrast representing the island's magnetic poles. The MFM images, with clear black and white sides to the islands, confirm the single-domain nature of the islands and easily resolve the individual magnetic orientations of the islands.

We first compare two very simple cluster geometries, shown in Fig. 1, the crosslike cluster we label F1 [Fig. 1(b)] and the looplike cluster NF6 [Fig. 1(c)]. As shown in Fig. 1(a), each of these clusters consists of four islands extracted from the square lattice of artificial spin ice. These two clusters provide limiting cases for situations of frustration (F1)

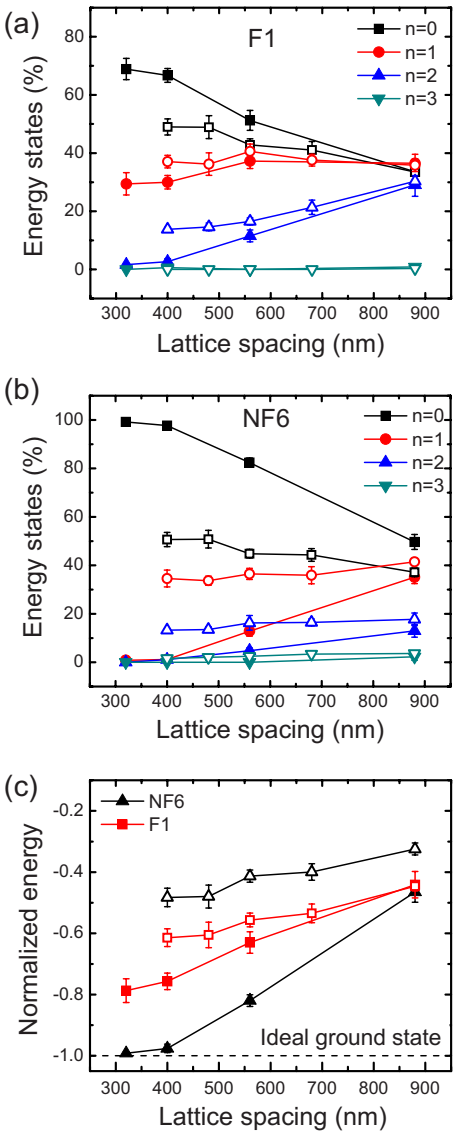

FIG. 3. (Color online) Populations of four energy states ($n=0,1,2,3$) for isolated cluster geometries (closed symbols) and for the same island configurations extracted from the extended lattice (open symbols) as a function of lattice spacing for (a) cluster F1 (cross) and (b) cluster NF6 (loop); (c) Normalized energy for these two cluster shapes, isolated clusters compared to the same island configurations extracted from extended lattice, the energies for the F1 and NF6 clusters are individually normalized to their respective ground-state energies.

and lack of frustration (NF6) between island moments. We define frustration in a cluster as the inability of all of the moments within it to simultaneously minimize the magnetostatic interactions of all the near-neighbor pairs (those pairs of islands that are separated by one square lattice spacing or less). The F1 geometry is frustrated because not all the pairwise near-neighbor interactions can be simultaneously minimized, whereas all near-neighbor interactions in the loop cluster NF6 can be minimized in a state where all of the moments point clockwise or counter clockwise around the loop. Under this definition, the frustrated clusters here all

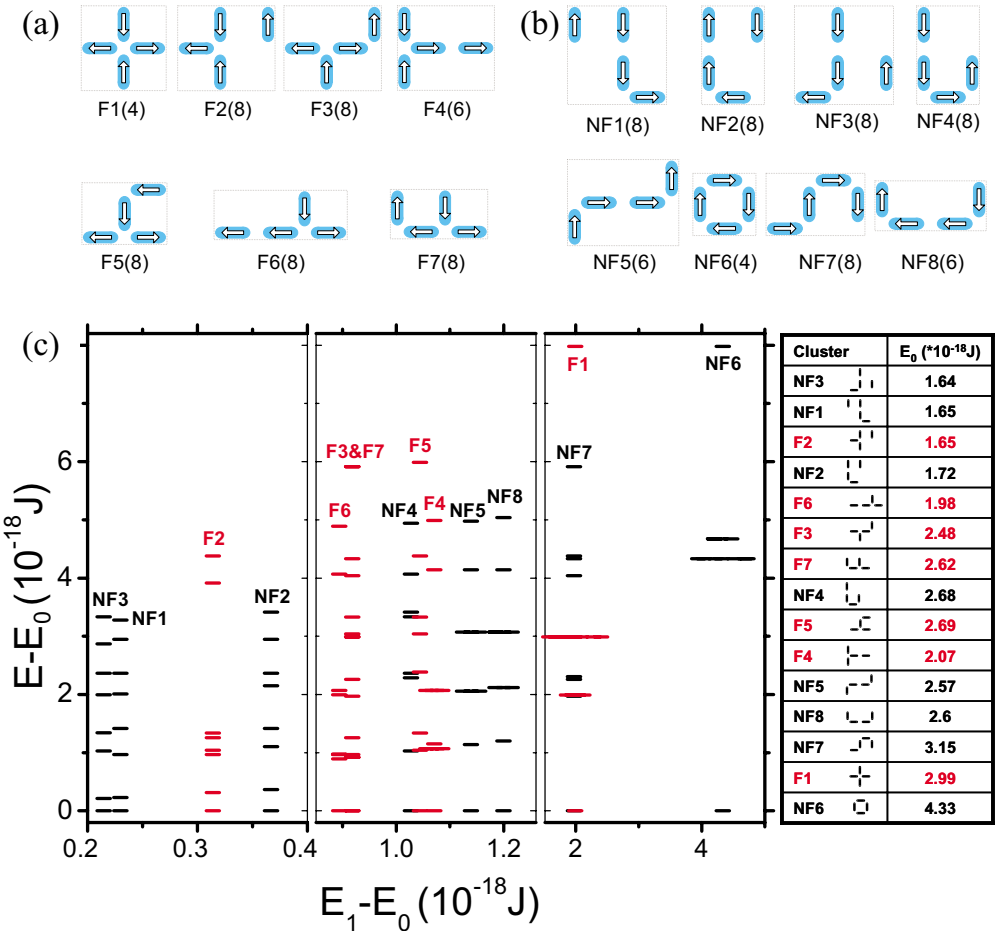

FIG. 4. (Color online) Schematic diagrams of cluster geometries (a) frustrated and (b) nonfrustrated. Arrows show one of the two ground-state configurations ($n=0$), and the number in the parenthesis is the total number of symmetry-distinct moment microstates (i.e., the total number of energy states, $n=0,1,2,\ldots$) for each geometry. (c) The energy spectra of the 15 geometries: energy levels $E-E_0$ obtained from micromagnetic simulation (Ref. 25) are plotted against the first energy spacing (E_1-E_0), the length of the line represents the degeneracy of this energy level; the table next to it shows the ground-state energy E_0 for each of the 15 cluster geometries in an order (from top to bottom) same as their appearance in this figure (from left to right).

contain a "T"-shaped motif of three islands, with the fourth in various possible positions.

We first examine the distinct island moment configurations and magnetostatic energies of the demagnetized clusters. The symmetry-distinct classes of moment configurations are microstates with well-defined magnetostatic energies that can be calculated by micromagnetic simulation using the OOMMF package.[25] We label the microstates by their relative energy from the ground state ($n=0$) to the highest energy configuration ($n=X$, where X is determined by the geometry of the cluster), as depicted in Figs. 2(a) and 2(b) for F1 and NF6, respectively. Both of these clusters have four symmetry-distinct classes of moment configurations (i.e., only four energetically distinct states), much reduced from the $2^4=16$ total configurations, because of the fourfold symmetry.

We obtain the populations of the different microstates and the average cluster energy from MFM images of large populations of isolated clusters as described above. Since F1 and NF6 are simply subsets of an extended square-ice lattice, the relative populations of corresponding $n=0$ through $n=X$ cluster states can also be obtained for the same island configurations extracted from the extended square-ice lattice (subject to the same demagnetization protocol). Figures 3(a) and 3(b) show the populations of the distinct cluster microstates as a function of interisland spacing for F1 and NF6, as compared to the corresponding populations from the extended lattice. All four cluster microstates for both F1 and NF6 follow the same overall trends with interisland spacing as do their counterparts extracted from the extended lattice. However, there are many more $n=0$ microstates in the clusters than in the corresponding lattice, showing that the ground state is more accessible in the isolated clusters than it is in the extended lattice. The average magnetostatic energy of the clusters versus lattice spacing (as determined by summing over measured populations, using the magnetostatic calculations for individual clusters mentioned earlier), shown in Fig. 3(c), reinforces the observation that it is easier for the isolated clusters to access lower energy states (the energy is individually normalized to the ground state in each case so that $E_0=-1$). The distinction between the populations of isolated clusters and those embedded in the lattice can be qualitatively understood as being due to the absence of competing interactions from neighboring islands outside the clusters.

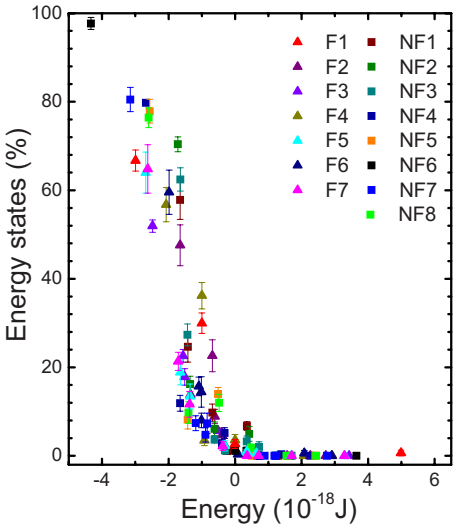

FIG. 5. (Color online) Percentages of all energy states ($n=0,1,2,\ldots$) for each cluster geometry as a function of the magnetostatic energy of this state [the energy of each state for each cluster geometry is calculated by OOMMF (Ref. 25)], the square and triangle symbols represent the nonfrustrated and frustrated clusters, respectively. The percentages of energy states are not normalized by the multiplicity of each state; however applying such a correction does not substantially change the overall behavior of the curve.

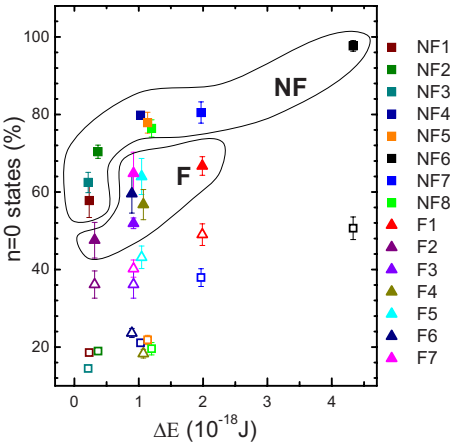

FIG. 6. (Color online) Percentages of $n=0$ energy states as a function of $\Delta E=E_1-E_0$ for all 15 cluster geometries. Closed symbols are for isolated clusters, and open symbols represent data for the same island configurations extracted from the extended lattice. Frustrated and nonfrustrated clusters are denoted, respectively, by triangles and squares, and are circled, respectively.

As seen in Fig. 3(c), the normalized cluster magnetostatic energy monotonically decreases with decreasing lattice spacing in all cases. Notably, the normalized energy of cluster NF6 approaches the value of E_0 at small interisland spacing, indicating that the ac demagnetization protocol enables this system to access its ground state in this limit. In contrast, the energy of cluster F1 fails to reach the ground-state value, instead achieving approximately −0.8 in normalized units. The frustrated cluster apparently has greater difficulty accessing its ground state, but we note that the presence or absence of frustration is not the only distinction between NF6 and F1 clusters, since the energies of the different moment configurations of the two clusters are also quite different. We can see this by considering the energy difference between the two lowest energy microstates of the moments, $\Delta E=E_1-E_0$, where E_1 and E_0 correspond to the magnetostatic energies of the $n=1$ and $n=0$ microstates. Comparing ΔE for F1 and NF6, we find that it is much smaller for F1 (1.99×10^{-18} J vs 4.33×10^{-18} J, or 1.4×10^{5} K vs 3.1×10^{5} K). We therefore note that it is possible that the difference in ground-state population could also be attributable to the relative energies of the different states of the clusters.

To isolate the effect of frustration from that of energy-level spacing, we study another 13 cluster geometries, as illustrated in Figs. 4(a) and 4(b), where the white arrows show the $n=0$ moment configuration for each cluster geometry. Using the same definition of frustration as before, these clusters can be separated into frustrated and nonfrustrated subsets, labeled F and NF accordingly in Figs. 4(a) and 4(b). The energy spectra for the 15 geometries are illustrated in Fig. 4(c): the energy levels $E-E_0$ are plotted against the first energy spacing ($\Delta E=E_1-E_0$) separately for each of the geometries. We see that the values of ΔE are similarly distributed and occupy approximately the same range of energies for both the frustrated and the nonfrustrated clusters. There is a weak tendency for frustrated clusters to have a higher degeneracy or near-degeneracy around the first excited state.

Because of differing degrees of symmetry, some cluster geometries have fewer symmetry-distinct cluster microstates than others. Figure 5 plots the populations of all symmetry-distinct cluster microstates as a function of their magnetostatic energy. For each of these geometries, the fractional population of the clusters is largest for the $n=0$ state and decays with increasing energy to approximately zero for the higher energy states (i.e., $n=2,3$). Although the overall behavior is roughly exponential, the data points for individual clusters do not precisely follow an exponential dependence, and the data thus do not warrant extraction of a characteristic energy scale. A direct comparison of the effects of frustration can be seen in Fig. 6, where the percentage of $n=0$ for each cluster is plotted against ΔE, and also compared to the percentage of $n=0$ extracted from the extended lattice. Just as for NF6 and F1 [see Figs. 2(a) and 2(b)], all cluster geometries have a much higher fractional population of $n=0$ than do their counterparts within the extended lattice. Importantly, the nonfrustrated isolated clusters consistently have a higher percentage of $n=0$ microstates than the frustrated isolated clusters with essentially the same ΔE, e.g., consider NF7 and F1. This trend strongly suggests that there is a distinct physical difference between frustrated and nonfrustrated cluster geometries, and the lack of distinction between their energy spectra in Fig. 4 as well as the effect appearing only in isolated clusters indicates that the difference originates in the frustration of the clusters. By moving far away from the infinite-size thermodynamic limit, these small clusters eliminate the macroscopic ground-state degeneracy that is characteristic of extended frustrated lattices. Hence the frustrated ground state of a small cluster no longer has a multiplicity advantage over unfrustrated systems, and its ground state becomes less accessible.

Our results suggest that frustration acts on the dynamics of ferromagnetic island clusters by providing a kinetic barrier that prevents the system from reaching lower energies. Understanding the details of this behavior will require considerable micromagnetic modeling, which is beyond the scope of the present work, but we can see that the nature of frustration is inherent in the energetic landscape of frustrated systems, even ones with such a finite extent as we are studying here. Our data suggest that one might obtain a detailed understanding of artificial spin ice systems by starting from small finite clusters and building to extended lattices. By building successively larger clusters, we should be able to extrapolate to the extended lattices and better understand the details of demagnetization, effective thermodynamics, and monopole excitations. Furthermore, the microstates of small clusters can be exhaustively enumerated, which opens the system to additional modes of analysis, as compared to extended systems, both in terms of effective thermodynamic treatments and (in the longer term) models of annealing kinetics.

We acknowledge financial support from the Army Research Office and the National Science Foundation MRSEC program (Grant No. DMR-0820404) and the National Nanotechnology Infrastructure Network. We are grateful to Chris Leighton and Mike Erickson for the film deposition.

*Corresponding author; pes12@psu.edu

[1] X. Ke, J. Li, C. Nisoli, P. E. Lammert, W. McConville, R. F. Wang, V. H. Crespi, and P. Schiffer, Phys. Rev. Lett. **101**, 037205 (2008).
[2] R. F. Wang, C. Nisoli, R. S. Freitas, J. Li, W. McConville, B. J. Cooley, M. S. Lund, N. Samarth, C. Leighton, V. H. Crespi, and P. Schiffer, Nature (London) **439**, 303 (2006); **446**, 102 (2007).
[3] R. F. Wang, J. Li, W. McConville, C. Nisoli, X. Ke, J. W. Freeland, V. Rose, M. Grimsditch, P. Lammert, V. H. Crespi, and P. Schiffer, J. Appl. Phys. **101**, 09J104 (2007).
[4] C. Nisoli, R. Wang, J. Li, W. F. McConville, P. E. Lammert, P. Schiffer, and V. H. Crespi, Phys. Rev. Lett. **98**, 217203 (2007).
[5] G. Möller and R. Moessner, Phys. Rev. Lett. **96**, 237202 (2006).
[6] A. Remhof, A. Schumann, A. Westphalen, H. Zabel, N. Mikuszeit, E. Y. Vedmedenko, T. Last, and U. Kunze, Phys. Rev. B **77**, 134409 (2008).
[7] J. Li, X. Ke, S. Zhang, D. Garand, C. Nisoli, P. Lammert, V. H. Crespi, and P. Schiffer, Phys. Rev. B **81**, 092406 (2010).
[8] P. E. Lammert, X. Ke, J. Li, C. Nisoli, D. M. Garand, V. H. Crespi, and P. Schiffer, Nat. Phys. (to be published).
[9] C. Nisoli, J. Li, X. Ke, D. M. Garand, P. Schiffer, and V. H. Crespi, Phys. Rev. Lett. **105**, 047205 (2010).
[10] Z. Budrikis, P. Politi, and R. L. Stamps, Phys. Rev. Lett. **105**, 017201 (2010).
[11] Y. Qi, T. Brintlinger, and J. Cumings, Phys. Rev. B **77**, 094418 (2008).
[12] M. Tanaka, E. Saitoh, H. Miyajima, T. Yamaoka, and Y. Iye, Phys. Rev. B **73**, 052411 (2006).
[13] A. Westphalen, A. Schumann, A. Remhof, H. Zabel, M. Karolak, B. Baxevanis, E. Y. Vedmedenko, T. Last, U. Kunze, and T. Eimuller, Phys. Rev. B **77**, 174407 (2008).
[14] S. Ladak, D. E. Read, G. K. Perkins, L. F. Cohen, and W. R. Branford, Nat. Phys. **6**, 359 (2010).
[15] P. Mellado, O. Petrova, Y. Shen, and O. Tchernyshyov, arXiv:1006.4075 (unpublished).
[16] X. Ke, J. Li, S. Zhang, C. Nisoli, V. H. Crespi, and P. Schiffer, Appl. Phys. Lett. **93**, 252504 (2008).
[17] Y. Han, Phys. Rev. E **80**, 051102 (2009).
[18] S. T. Bramwell and M. J. P. Gingras, Science **294**, 1495 (2001).
[19] E. Mengotti, L. J. Heyderman, A. Fraile Rodriguez, A. Bisig, L. Le Guyader, F. Nolting, and H. B. Braun, Phys. Rev. B **78**, 144402 (2008).
[20] R. P. Cowburn and M. E. Welland, Science **287**, 1466 (2000).
[21] D. B. Carlton, N. C. Emley, E. Tuchfeld, and J. Bokor, Nano Lett. **8**, 4173 (2008).
[22] A. Imre, G. Csaba, L. Ji, A. Orlov, G. H. Bernstein, and W. Porod, Science **311**, 205 (2006).
[23] H. T. Diep, *Frustrated Spin Systems* (World Scientific, New York, 2005).
[24] R. Baxter, *Exactly Solved Models in Statistical Physics* (Academic, New York, 1982).
[25] OOMMF NIST code, http://math.nist.gov/oommf (2005).